

ANN approaches to determine the dielectric strength improvement of MgO based low density polyethylene nanocomposite

Sherif Haggag^{*,‡}, Loai Nasrat^{†,§} and Hanafy Ismail^{*,¶}

^{*}Faculty of Engineering, Department of Power and Machines
Ain Shams University, Cairo, Egypt

[†]Faculty of Engineering
Department of Electrical Engineering Aswan University, Aswan, Egypt

[‡]Sh.h.haggag@gmail.com

[§]Loaisaad@yahoo.com

[¶]Hanafy_22356@hotmail.com

Received 22 March 2021; Revised 26 April 2021; Accepted 12 May 2021; Published 23 June 2021

This paper presents the modification occurred to the dielectric strength feature of low density polyethylene compounded with nano magnesia (LDPE/MgO). MgO nanoparticles were prepared using sol-gel technique, MgO filler surface was functionalized to improve the interfacial bonding. Specimen's groups of composites with different filler concentrations were fabricated by mix blend method. Samples exposed to various salinity media by immersion, dielectric strength test was applied on each set according to relevant ASTM standard with identical testing technique. The results were statistically processed then compared to the pristine material. Tests results utilized to learn Artificial Neural Network in order to acquire the value of dielectric strength of compounds having similar composition but containing different doping amounts or influenced with various salinity level media. The dielectric strength is enhanced by the addition of MgO nanofiller. From the investigation of the obtained results, it is concluded that additives of 1.4% filler concentration by weight is the optimum MgO content for LDPE/MgO nanofiller material. We think that this paper may promote a good researching methodology that gather both empirical work and numerical tools in this field.

Keywords: Polymer nanocomposites; salinity; surface treatment; breakdown strength; artificial neural network.

1. Introduction

Polymer composites and blends in dielectric applications have lately garnered significant interest of researchers.¹⁻³ The applicability of customizing polymers features to suit particular objectives met approbation by the industrial sector. In electrical insulation field, polymers nanocomposites which also known as nanodielectrics,⁴ is considered an evolutionary leap. Adding few grams of nanoparticles can improve insulation characterization of the polymeric materials.

Low-density polyethylene and nanomagnesia composite is famous and has been under scientific investigation recently where it proved that it can provide premium material enhancement to the HVDC cables insulation.⁵

Space charges suppression,⁶ volume resistivity augmentation,⁷ dielectric strength improvement,⁸ lessening electric treeing inception and treeing diffusion repression⁹ are some of the advantages that could be acquired by utilizing LDPE-MgO composites in cables insulation manufacturing.

In reality, cables are still transmitting HVAC and placed underground in different media other than the ideal

conditions. Salty media, located in places like soils of dry areas or coastal areas or those exposed to snow melting, is one of the external parameters impacting insulation functionality of the direct buried HV cables.¹⁰

In order to identify the development of the dielectric properties achieved by nanocompositing process in more practical conditions, MgO Nanoparticles were prepared using sol-gel technique,¹¹ particles surface was modified using silane coupling agent¹² then, sample's sets of composites with different filler weight concentrations were prepared and exposed to simulated media having various salinity levels by immersion, each set was examined according to relevant standard while preserving identical testing parameters and similar external conditions. The results were compared to the pristine material.

Due to the shortage of the empirical outcomes resulted from the cost impact of the materials consumed and equipment employed during the experiments; also, the difficulties confronted in the laboratories, an approach of developing an artificial neural network that is capable of forecasting the

[‡]Corresponding author.

dielectric strength of composites of any filler doping value or submerged in salty medium was found to be fruitful.

2. Experimental Work

2.1. Materials and treatments

Natural resin, ultra-pure LDPE of 0.924 g/cm³ density and 2.00 g/10 min melt flow rate at 190 °C & 2.16 kg load was purchased in granules form from SABIC, KSA then grounded to powder with average particles diameter of less than 0.2 mm for better amalgamation.

MgO fine particles were fabricated in-house. Synthesis of magnesia is achieved using bottom-up, sol-gel technique by hydrolysis of the Magnesium Chloride, Hexahydrate precursor in presence of Triton X₁₀₀, nonionic surfactant. Final product was in average diameter size of 70 ± 10 nm. (MgCl₂·6H₂O) manufactured by El Nasr Pharmaceutical Chemicals Co., Egypt.

MgO is a promising filler thanks to its wide bandgap of (7.8 eV); also, MgO owns the most significant volume resistivity value compared to other ordinarily used nanooxides. Moreover, it is a relatively cheap nanomaterial.

Regarding surface characterization of nanomagnesia, two phases processes were adopted for better surface characterization of the filler.

The first stage is the acidic etching which aims to increase the hydroxyls tails of the nano-MgO surface as a preparation step for modifier loading.

Second step is to apply the silane coupling agent for the compatibilism of the filler that has hydrophilic nature with the hydrophobic base polymer and consequently enhancing the filler-matrix cohesion. 5 wt.% of Hexadecyltrimethoxy silane from Sigma Aldrich, Germany, was added for particles loading.

Percentage of the used silane was purposed according to Ref. 13.

2.2. Nanocomposites preparation

The particles must be integrated into the base material in a way leading to an isolated, well-dispersed primary nanoparticle inside the matrix with high homogeneity and minimal-agglomeration.

Melt Blending, a direct mixing technique, is utilized to prepare the required composite in which shear stresses are applied to the melted polymer in the presence of the filler, causing homogenous distribution of the filler in the polymeric host matrix.

Direct mixing of LDPE & nano-MgO was done using (Brabender Lab Station) twin extruder, with rotational screws speed of 15 rpm and spinning torque of 28 Nm while heating temperature was almost 170 °C. The melted composite provided by the extruder is quenched in a water bath before being granulated using speed controlled pelletizer machine (Brabender Granulator S).

Outcome composite was softened using roller milling machine (LAB TECH), rolls temperature settings were 160 °C and 145 °C with rotating speed of 10 rpm for both while the gap between them is adjusted to be 0.5 mm. Molten composite produced was compressed gradually by sheet pressing machine (Gibitre Lab Press) to eliminate any air bubbles in the produced sheet. The finally fabricated sheet is of 200 × 200 mm dimensions and around 1-mm thickness.

Samples' preparation was done in R&D labs at EGYPLAST factory, El Sewedy Group, Egypt.

The sequence of MgO nanoparticles preparation process is depicted by the flowchart in Fig. 1.

The chemical reactions occurred during nanomagnesia characterization phase are illustrated in Fig. 2.

Several composite sheets with various filler loads were fabricated so as to apply intended tests to them.

Table 1 presents the filler percentage doped in LDPE polymer.

2.3. Stepwise morphology characterization

T Philips X'pert X-ray Diffraction (XRD) was utilized to ensure the crystallinity phase and purity of the synthesized nanoparticles.

Nicolet 6700 Fourier Transform Infrared (FTIR) Spectrometer was used with common 4000–400 cm⁻¹ region to ensure the presence of hydroxyl group forming hydrophobic tail in surface modification stage. FTIR was done before and after modifying the MgO fine particles surface to compare between them.

TEM was performed on JEOL JEM-2100 high resolution transmission electron microscope at an accelerating voltage of 200 kV to check the shape and size of the fabricated nanoparticles.

SEM captures were taken for composites by JEOL JSM 5400 LV Scanning Electron Microscopy to examine the uniform diffusion of the filler.

XRD was performed at X-Ray center at Faculty of Science, Ain Shams University, whereas both FTIR and TEM were done at Nanotech Egypt Laboratories.

- (1) **XRD:** The pattern provides the structure of the cubic phase of MgO. The comparison between X-ray diffraction pattern peaks of the fabricated MgO and their counterpart of the cubic MgO standardized in Ref. 14, mp-1265, presented in Figs. 3(a) and 3(b), respectively shows matching that assures the purity and homogeneity of the final product obtained.
- (2) **FTIR:** Spectrum captured before and after nano-MgO surface characterization stage is introduced in Fig. 4. A peak with sharp appearance is clearly noticed at 3696 cm⁻¹ of the surface modified oxide, reflecting the presence of typical OH stretching bonds of hydroxyl.
- (3) **TEM:** MgO synthesized is of white powder appearance, TEM photos proved that the average diameter size

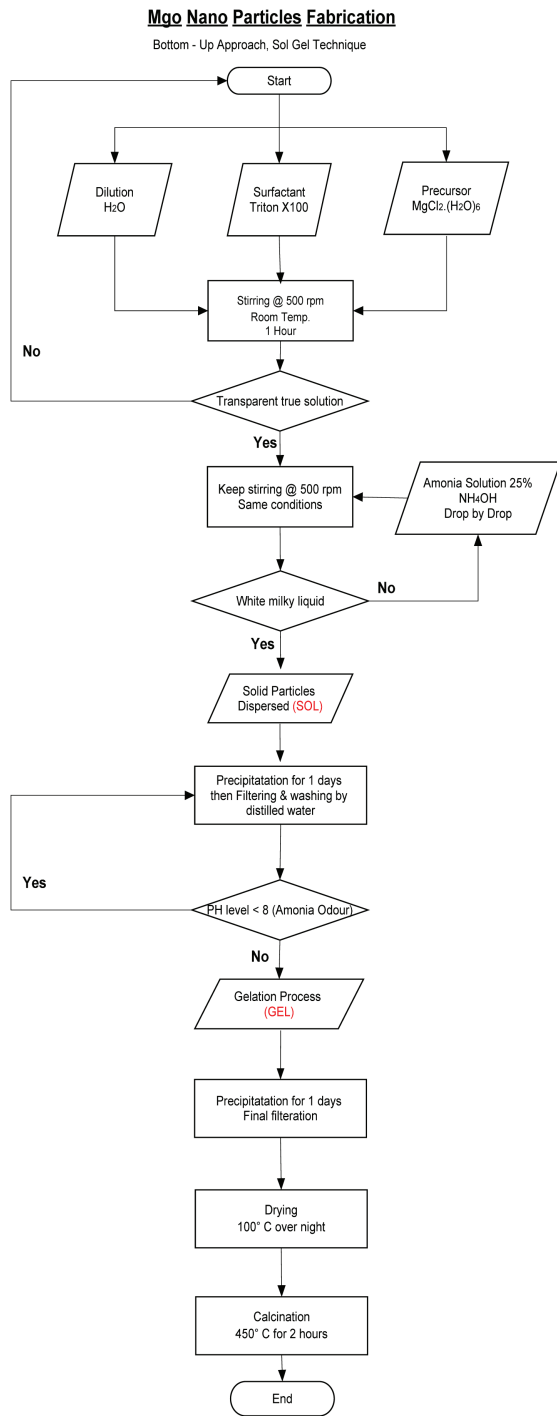


Fig. 1. MgO nanoparticles preparation process.

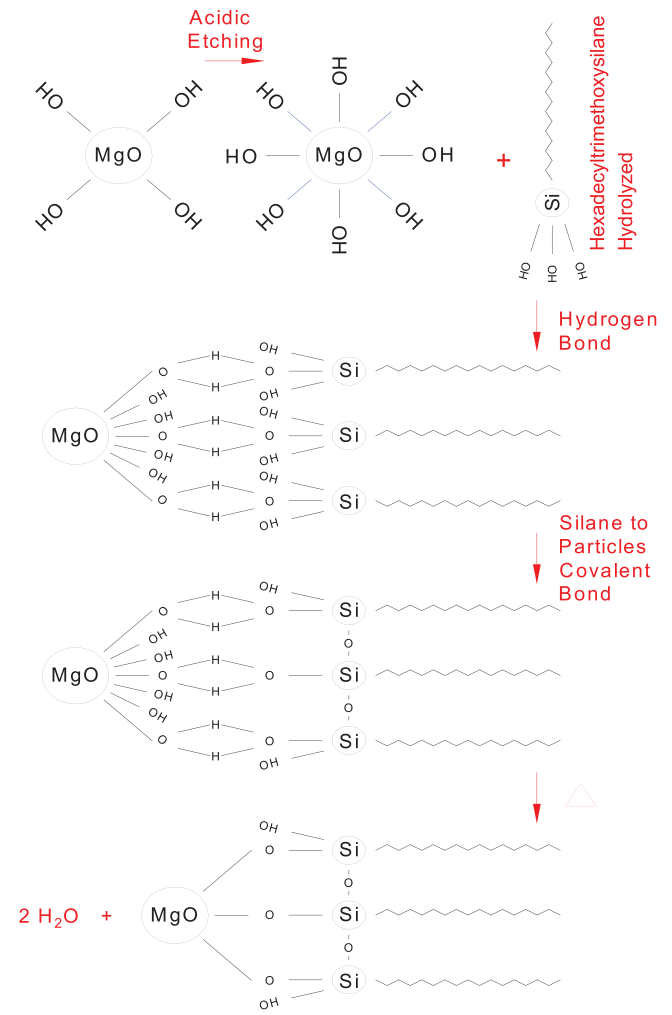


Fig. 2. MgO nanoparticles characterization.

Table 1. Different samples compositions.

Sample	Tag	LDPE (wt.%)	Nano-MgO (wt.%)
LDPE	P	100	0
LDPE + 0.5% MgO	N1	99.5	0.5
LDPE + 1.0% MgO	N2	99	1
LDPE + 1.5% MgO	N3	98.5	1.5
LDPE + 2.5% MgO	N4	97.5	2.5
LDPE + 4.0% MgO	N5	96	4

measured is 75 ± 10 nm. Particles configured to be a mixture of spherical and quasi-spherical shapes. Figures 5(a) and 5(b) are the TEM images taken.

- (4) **SEM:** Shot images ensured the good dispersion of the filler particle in the host matrix on low loading levels of 1wt.%, while aggregations were noticed at higher loading degrees of 4 wt.%.

2.4. Dielectric strength test

Dielectric strength was tested according to ASTM D-149 using TERCO instrument kits, Sweden, portrayed in Fig. 7. Test Specimens were cut in disc shape of diameter not less than 5 cm and thickness > 1 mm. For each filler concentration

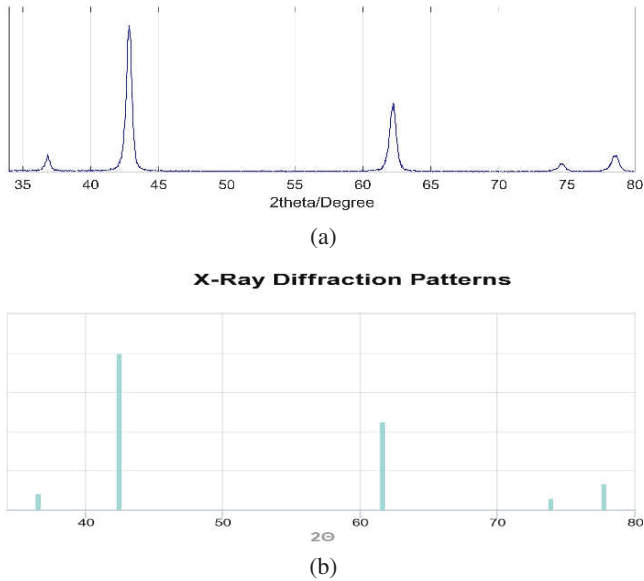


Fig. 3. (a) XRD of fabricated MgO. (b) Standard MgO XRD mp-1265.

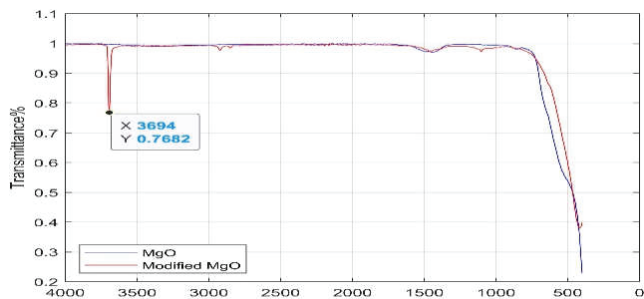


Fig. 4. FTIR of MgO and modified MgO.

prepared, 10 samples were clipped and tested, extreme value statistics were applied to each population's results afterward.

Tests were done in HV laboratory at Faculty of Engineering, Aswan University.

Dielectric strength test was performed on all specimens, P and N1–N5, with diversified testing conditions to examine the impact of different media with salinity that insulation might accommodate them. Test aims to determine the influence of the dissolved salt presence with different levels on the degradation of the insulation property

In this context, separate groups of specimens were tested in the following media conditions:

- Group A was tested by AC voltage; samples were in dry condition.
- Group B was tested by AC voltage; samples were immersed in solution of zero salinity.
- Group C was tested by AC voltage; samples were immersed in solution of 5 mS/cm salinity.

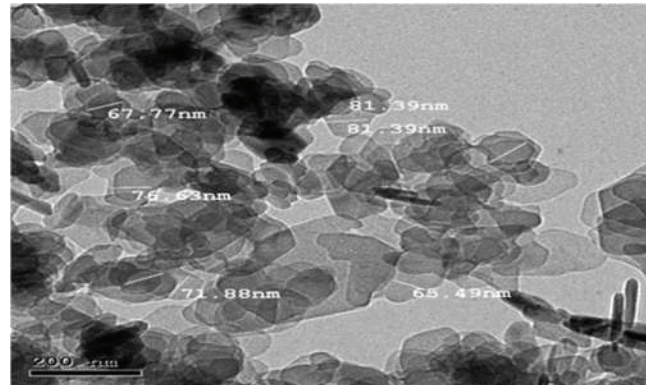
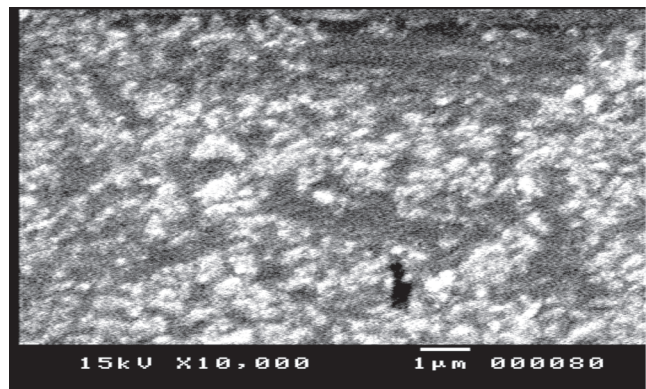
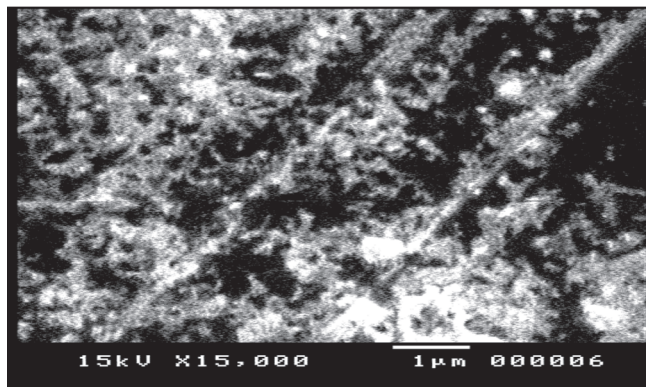


Fig. 5. MgO nanoparticles TEM captures.



(a)



(b)

Fig. 6 (a) LDPE-nano-MgO capture at 1 wt.% filler loading. (b) LDPE-nano-MgO capture at 4 wt.% filler loading.

- Group D was tested by AC voltage; samples were immersed in solution of 10 mS/cm salinity.
- Group E was tested by AC voltage; samples were immersed in solution of 15 mS/cm salinity.
- Group F was tested by AC voltage; samples were immersed in solution of 20 mS/cm salinity.

LDPE–MgO composites discs were kept clean and dried without any accumulated dust or any other foreign contamination on the face prior to Group A testing.

For group B, wet test preparation was done with reference to ASTM D-570, in which specimens were totally submerged in distilled water for 24 h at room temperature, removed, and dried by a rag before being tested.

As for Groups C–F, Salty wet test preparations are typical to that of Group B yet, specimens immersed in salty water of 5, 10, 15 and 20 mS/cm, respectively.

Immerging bathes were made by dissolving certain amounts of sodium chloride (NaCl) into distilled water with stirring. Salinity unit is milli-siemens per centimeter was measured using Electrical Conductivity Tester recursively to tune the salinity.

Dielectric strength was obtained by rising up the external field by 2 kV/s rate then automatically record the maximum potential reached over the sample before breakdown occurs using the formula in Eq. (1)¹⁵:

$$E = V/d, \tag{1}$$

where:

- E*: Dielectric Strength kV/mm
- V*: Maximum potential detected before breakdown kV
- d*: Sample thickness.

Weibull statistical function is employed to analyze the tested population data. Two parameters Weibull formula might be expressed as in Eq. (2)

$$P(E) = 1 - \exp\left[-\left(\frac{E}{\alpha}\right)^\beta\right], \tag{2}$$

where,

- E*: Expermintally recorded Dielectric Strength kV/mm
- P(E)*: Cumulative breakdown failure probability
- α : Breakdown gradient at failer probability of 63.2%
- β : Shape Parameter.

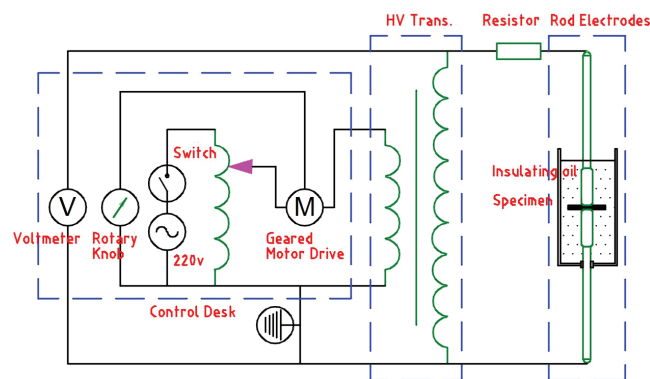


Fig. 7. Dielectric strength testing circuit.

For a population of less than 20 specimens ($n < 20$), the i th cumulative probability (P_i) related to the i th sample of breakdown incident (i) is obtained using IEC 62539 standard approximation shown in Eq. (3)

$$P_i = \frac{i - 0.44}{n + 0.255}, \tag{3}$$

Least square method of linear regression technique was used to evaluate α and β Weibull variables.

2.5. Artificial neural network

Artificial Neural Network is used to anticipate the dielectric strength level corresponding to LDPE/MgO composites having any nano-MgO filler concentration and placed in any degree of salty medium.

Feed Forward, Backpropagation network type was chosen for its simplicity, popularity and accuracy. The two inputs of the proposed network are the filler percentage and salinity level in mS/cm, while the output is the foreseen value of the dielectric strength in kV/mm. The network contains five hidden layers. ANN structure is illustrated in Fig. 8.

Network training has been done using the actual results obtained experimentally; however, one result out of each group was saved away from the learning band to be used as a checker in order to validate the algorithm.

Mean Square Error was chosen as the performance function, Sigmoid was selected as an activation function, learning rate was adjusted to 0.5 and random initial weights were given to the network.

Backpropagation weight modifier adopts a reversed calculation pass in which inputs are applied in the usual forward pass; the obtained error is analyzed by derivative function, sign, and magnitude of the substitution guides to update the weights in each iteration till an acceptable error percentage is reached.

3. Results and Discussion

3.1. Dielectric strength tests results

Dielectric strength tests conducted on groups A–F of the prepared LDPE–MgO nanocomposites specimens, results were recorded.

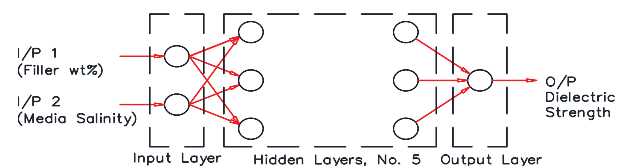


Fig. 8. ANN structure.

Table 2. Characteristic dielectric strength and related shape parameter.

Group	Unit	Filler wt. %					
		0.00	0.50	1.00	1.50	2.50	4.00
A	kV/mm	26.15	30.76	36.83	38.13	34.03	30.89
	β	1.69	0.69	1.80	1.35	2.39	1.50
B	kV/mm	23.83	26.14	36.43	36.37	32.94	28.96
	β	1.39	2.09	0.57	1.19	0.77	1.73
C	kV/mm	20.92	24.97	33.66	33.64	29.62	26.77
	β	2.08	1.31	1.15	2.33	1.03	1.09
D	kV/mm	20.05	23.29	32.96	32.99	29.13	25.73
	β	1.23	1.15	0.55	1.21	1.25	2.42
E	kV/mm	19.31	21.80	31.76	31.37	27.25	26.16
	β	2.35	2.86	1.08	1.70	3.81	1.02
F	kV/mm	18.76	21.61	30.27	31.03	27.42	25.07
	β	3.27	2.08	3.76	2.10	2.05	1.64

Figures 9(A)–9(F) represent the cumulative probability of AC breakdown strength of neat LDPE and LDPE/MgO nanocomposites, and a summarization of characteristic dielectric strength with related shape parameter are in Table 2.

Matlab was utilized to interpolate the results obtained where Makima interpolation function is selected¹⁶; in addition, maximum dielectric strength could be anticipated from the plot of each conditional group.

The patterns of all groups were found to be almost typical, forming skewed bell shapes, as shown in Fig. 10. It could be seen that the breakdown voltage increases gradually with the augmentation of the nanofiller till the filler percentage reached around 1.5%, then they start to decline with higher filler concentrations.

Generally, in low frequencies spectrum, solid polymer breakdown voltage shrinks with higher frequencies by the effect of the dielectric losses that induce internal heating in the insulation, hence, make it easier to break at lower voltages.^{17,18}

Results could be interpreted as, up to around 1.5% filler percentage, dielectric strength is modified progressively with rising the doping amount. This observation might be justified by checking the surface group polarization, which, in nanoscale, has a predominant effect on all other dipolar groups.

By applying an external electric field, nanofiller surface group ionized, releasing free negatively charged electrons and positive molecular ions. The density of those charged elements is directly proportional to the filler ratio; therefore, with low particles concentrations, emitted electrons and ions numbers are low, oppositely, the interface of inorganic nanoparticles to the base material matrix causing a mutation to its crystallinity. Particles adhered to the host lattice through

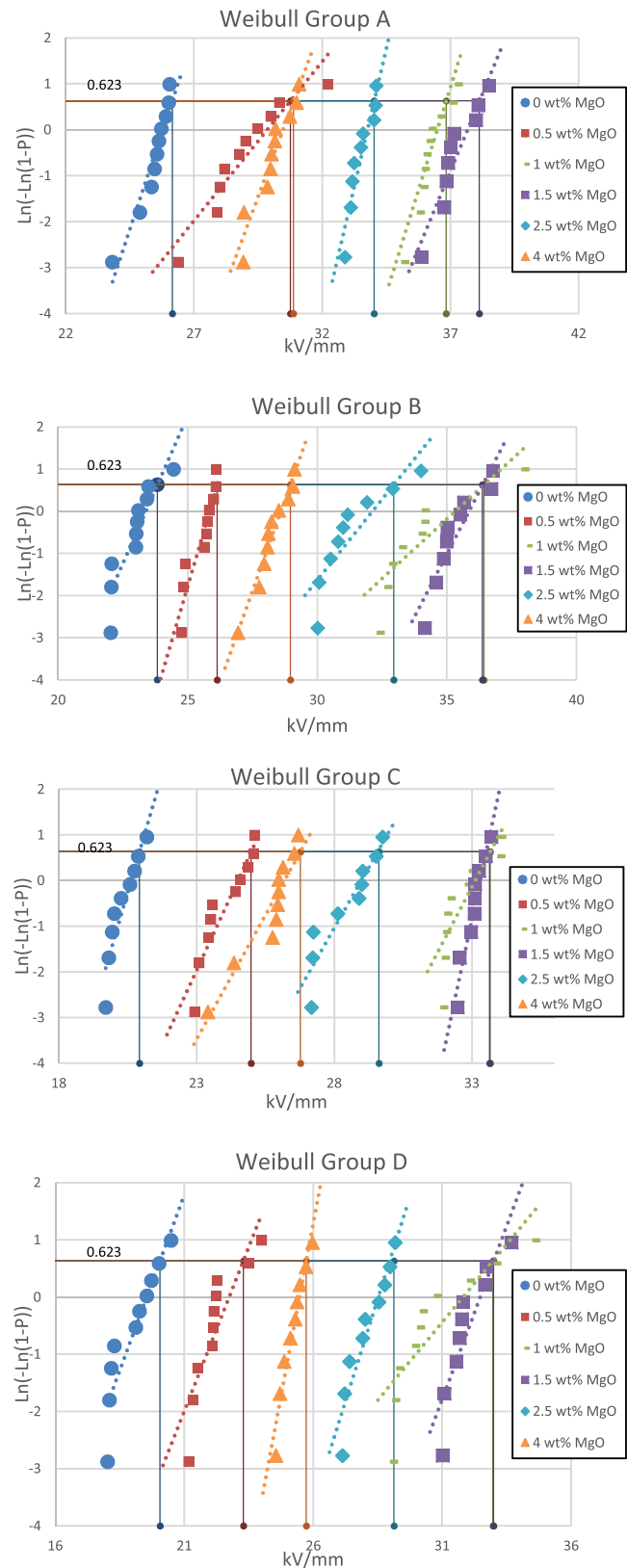


Fig. 9. Weibull distribution for groups (A–F).

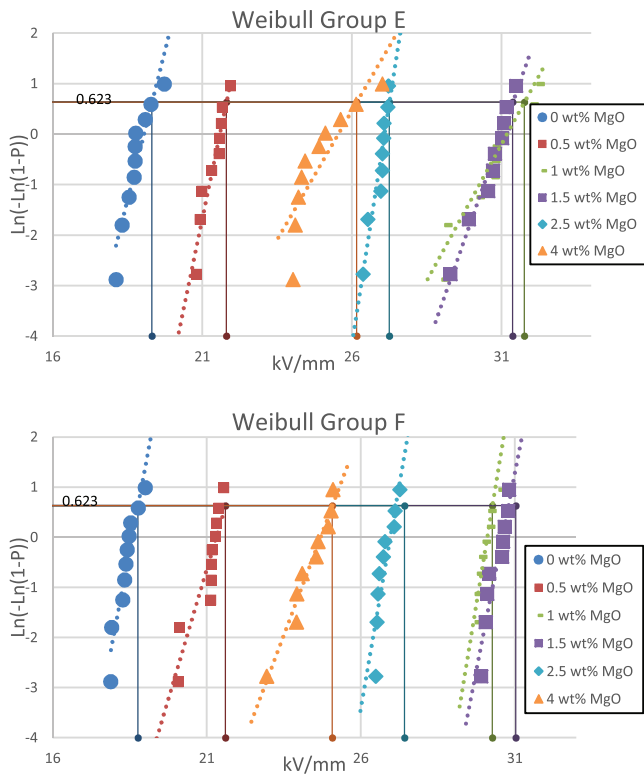


Fig. 9. (Continued)

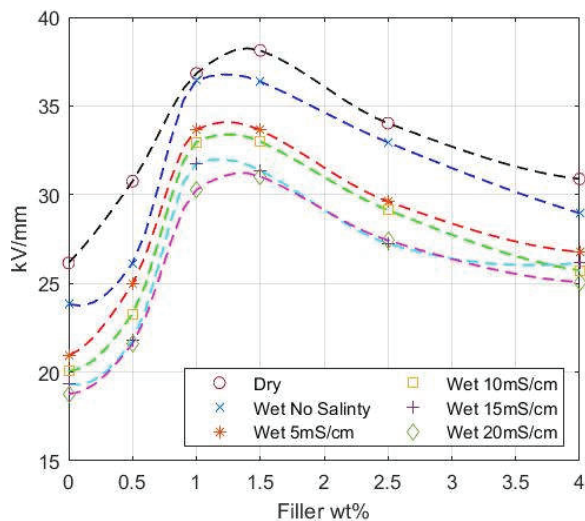


Fig. 10. Different salinity levels impact on LDPE-MgO dielectric strength.

the doping process could be considered as impurities that manipulate the original structure; consequently, considerable number of traps of different depths are formed that would restrain the mobility of the charged elements. As a result, the breakdown voltage is gradually enhanced.^{19,20}

With higher concentration levels of nanofiller, surface modification procedures taken are no more capable of

Table 3. Group max. dielectric strength and related filler ratio.

Condition	Tag	Max. kV/mm	Filler (wt.%) at Max kV/mm
Dry	Group A	38.25	1.4
Wet	Group B	36.77	1.2
Wet, 5 mS/cm Salinity	Group C	34.08	1.2
Wet, 10 mS/cm Salinity	Group D	33.15	1.3
Wet, 15 mS/cm Salinity	Group E	32.25	1.2
Wet, 20 mS/cm Salinity	Group F	31.41	1.4

preventing the particle’s agglomeration. By adding more filler percentages, particles aggregates, creating bigger size MgO clusters. Interfacial adherence between hosting polymer and nanoparticles, which was the main reason of the homogeneous dispersion inside the matrix is overwhelmed by the surface energy raised by the increased loading. Such aggregates cause nonuniformity and distortion in the internal electric field, consequently, reduction in dielectric strength.

Moreover, it could be observed that salinity level is inversely proportional to the dielectric strength value. Dielectric strength of the optimum filler ratio diminishes exponentially with salinity incrimination.

Table 3 presents the peak of each group together with the corresponding filler weight ratio acquired.

The behavior of dielectric strength can be rationalized through the presence of dissociated ions surrounded by water solvation shells inside the LDPE matrix after soaking. In particular, dissociated Na⁺ and Cl⁻ are expected to be encapsulated in polar water cages. The presence of such polar media inside the polymer matrix, especially near the surface, could provide a percolation path for electronic transport, reducing the breakdown voltage of the composite.^{21,22}

Dielectric Strength decays linearly with low salinity levels, and in mediums of higher salt contamination amounts; it tends to saturate, as noticed from Table 3 values.

Figure 11 introduces salinity levels impacts on LDPE–MgO dielectric strength.

3.2. Feed forward artificial neural network

Exercising the proposed Artificial Neural Network with backpropagation proved to be a successful approach. The network has been trained well over the iterations run, providing a prediction to the value of dielectric breakdown as an output. ANN outcome error was calculated by the equation

$$\text{Error Percentage} = \frac{|\text{Experimental value} - \text{FFNN value}|}{\text{Experimental value}} * 100.$$

As a verification, checker point of each studied condition was omitted from the training process; instead, those saved

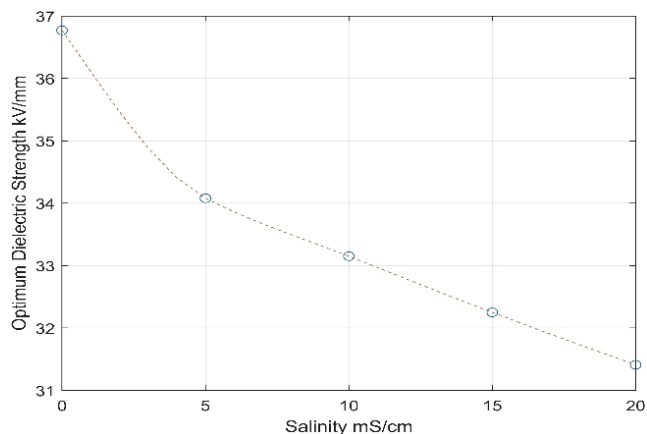


Fig. 11. Different salinity levels impact on LDPE–MgO dielectric strength.

assets were used as inputs then applied to the network to validate the ANN algorithm.

Table 4 introduces the two I/Ps in the first two columns cells, actual experimental results of dielectric strength value, predicted values obtained by the algorithm, and calculated error percentages, while underlined bold ones show checker values used, relevant output and error percentage.

The empirical values and ANN estimation were graphically represented in Fig. 12.

Results show an acceptable error percentage where the greatest error value of all concentrations in all cases did not exceed 4%, which evidence the achievement of the intended purpose.

Moreover, filler ratios corresponding to maximum dielectric strength of all tested groups, which were attained from the interpolating experimental results were experienced on the ANN algorithm. As demonstrated in Table 5, the difference

Table 4. FFANN inputs, output and error percentage.

Sr.	Filler loading (%) [I/P 1]	Test condition [I/P 2]	Lab. results kV/mm	NN estimation [O/P]	Error percent. (%)
1	0	Dry	26.153	25.719	1.658
2	0.5		30.760	29.988	2.508
3	1		36.830	35.296	4.167
4	1.5		38.126	37.247	2.306
5	2.5		34.028	33.991	0.108
6	4		30.885	30.772	0.367
7	0	Wet	23.827	23.687	0.588
8	0.5		26.140	25.517	2.387
9	1		36.429	35.775	1.797
10	1.5		36.373	36.322	0.140
11	2.5		32.944	32.482	1.405
12	4		28.957	28.518	1.516
13	0	5 mS/cm salinity	20.918	20.747	0.817
14	0.5		24.974	24.085	3.562
15	1		33.664	32.859	2.391
16	1.5		33.636	32.754	2.622
17	2.5		29.616	29.160	1.539
18	4		26.767	26.751	0.060
19	0	10 mS/cm salinity	20.053	19.409	3.215
20	0.5		23.286	23.025	1.124
21	1		32.962	32.737	0.684
22	1.5		32.992	32.404	1.781
23	2.5		29.126	28.969	0.538
24	4		25.725	25.560	0.644
25	0	15 mS/cm salinity	19.314	18.978	1.738
26	0.5		21.797	21.457	1.561
27	1		31.757	31.165	1.865

(Continued)

Table 4. (Continued)

Sr.	Filler loading (%) [I/P 1]	Test condition [I/P 2]	Lab. results kV/mm	NN estimation [O/P]	Error percent. (%)
28	1.5	15 mS/cm salinity	31.368	31.275	0.298
29	2.5		27.249	26.585	2.434
30	4		26.160	26.131	0.109
31	0	20 mS/cm salinity	18.762	18.657	0.559
32	0.5		21.609	21.457	0.705
33	1		30.275	30.018	0.847
34	1.5		31.030	30.801	0.739
35	2.5		27.420	27.329	0.332
36	4		25.075	25.034	0.161

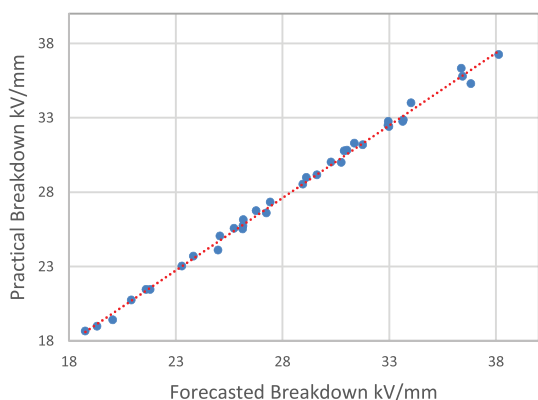


Fig. 12. Graphical presentation to ANN prediction versus lab. findings.

Table 5. Interpolation and ANN values of max dielectric strength in each group.

Tag	Filler %	Interpolation max. kV/mm	Max. kV/mm anticipated by ANN	Difference %
Group A	1.4	38.25	37.43	2.16
Group B	1.2	36.77	35.70	2.91
Group C	1.2	34.08	33.89	0.55
Group D	1.3	33.15	32.84	0.94
Group E	1.2	32.25	31.88	1.15
Group F	1.4	31.41	31.09	1.02

percentage among all groups did not exceed 3% with respect to the interpolation values.

4. Conclusion

In this research, dielectric strength properties of different weight ratios of nano-MgO compounded to LDPE were tested

in dry, wet and wet with different salinity levels impact; the results were used to train an ANN to anticipate any require dielectric value not physically obtained. The conclusions are summed up as follows

- (a) Pristine LDPE shows the lowest dielectric strength in all concentrations, which clearly indicates that doping LDPE with Nano-MgO resulting in significant modification of its insulation properties.
- (b) Dielectric strength behavior in all tested cases is similar. Below filler concentrations of about 1.5%, dielectric strength is increasing, while after this value, it decays exponentially till it saturates.
- (c) Salinity value impacting in an inverse proportional manner to the dielectric strength of the LDPE/MgO nanocomposite.
- (d) ANN exploits the experimental results for proper training; it managed to estimate dielectric strength values with high accuracy.

Acknowledgment

The authors gratefully acknowledge Faculty of Science, Ain Shams university, Faculty of Engineering, Aswan University, and Egyplast Factory R&D section (El Sewedy Group) for their cooperation and contribution to this work.

References

¹X. He, J. Zhou, L. Jin, X. Long, H. Wu, L. Xu, Y. Gong and W. Zhou, Improved dielectric properties of thermoplastic polyurethane elastomer filled with core-shell structured PDA@TiC particles, *Materials* **15**, 13 (2020).

²Y. Zhou, J. Hu, B. Dang and J. He, Titanium oxide nanoparticle increases shallow traps to suppress space charge accumulation in polypropylene dielectrics, *RSC Adv.* **6**(54), 48720–48727 (2016).

³J. Parameswaranpillai, S. Thomas and Y. Grohens, *Characterization of Polymer Blends: Miscibility, Morphology, and Interfaces*, 1st edn., eds. S. Thomas, Y. Grohens and P. Jyotishkumar (Wiley-VCH, 2015), pp. 1–5.

- ⁴L. S. Schadler and J. K. Nelson, Polymer nanodielectrics - Short history and future perspective, *J. Appl. Phys.* **128**, 12 (2020).
- ⁵L. K. H. Pallon, A. T. Hoang, A. M. Pourrahimi, M. S. Hedenqvist, F. Nilsson, S. Gubanski, U. W. Geddea and R. T. Olsson, The impact of MgO nanoparticle interface in ultra-insulating polyethylene nanocomposites for high voltage DC cables, *J. Mater. Chem. A* **4**(22), 8481–8916 (2016).
- ⁶Y. Hayse, H. Aoyama, K. Matsui, Y. Tanaka, T. Takada and Y. Murata, Space charge formation in LDPE/MgO nano-composite film under ultra-high DC electric stress, *IEEE Trans. FM* **126**(11), 1084–1089 (2006).
- ⁷Y. Murakami, M. Nemoto, S. Okuzumi, S. Masuda, M. Nagao, N. Hozumi and Y. Sekiguchi, DC conduction and electrical breakdown of MgO/LDPE nanocomposite, *IEEE Trans. Dielectr. Electr. Insul.* **15**(1), 33–39 (2008).
- ⁸S. Peng, J. He, J. Hu, X. Huang and P. Jiang, Influence of functionalized MgO nanoparticles on electrical properties of polyethylene nanocomposites, *IEEE Trans. Dielectr. Electr. Insul.* **22**(3), 1512–1519 (2015).
- ⁹Y. Murata, Y. Sekiguchi, Y. Inoue and M. Kanaoka, Investigation of electrical phenomena of inorganic-filler/LDPE nanocomposite material, *Int. Symp. Electr. Insulating Materials (ISEIM)*, Vol. 3 (2005), pp. 650–653.
- ¹⁰A. Bojovschi, T. V. Quoc, H. N. Trung, D. T. Quang and T. C. Le, Environmental effects on HV dielectric materials and related sensing technologies, *Appl. Sci.* **9**(5), 2–15 (2019).
- ¹¹F. Z. Haque, R. Nandanwar and P. Singh, Evaluating photodegradation properties of anatase and rutile TiO₂ nanoparticles for organic compounds, *Optik* **128**(10), 191–200 (2017).
- ¹²N. M. K. Abdel-Gawad, D. A. Mansour, A. Z. ElDein, H. M. Ahmed and M. M. F. Darwish, Effect of functionalized TiO₂ nanoparticles on dielectric properties of PVC nanocomposites used in electrical insulating cables, *MEPCON* **18**, 693–698 (2016).
- ¹³H.-S. Jung, D.-S. Moon and J.-K. Lee, Quantitative analysis and efficient surface modification of silica nanoparticles, *J. Nanomater.* **2012**, 1–8 (2012).
- ¹⁴<https://materialsproject.org/materials/mp-1265/>.
- ¹⁵S. Z. A. Dabbak, H. A. I. B. C. Ang, N. A. A. Latiff and M. Z. H. Makmud, Electrical properties of polyethylene/polypropylene compounds for high-voltage insulation, *Energies* **1148**(11), 6 (2018).
- ¹⁶The Mathworks Inc., Matlab, R2020b [computer program] (2020).
- ¹⁷S. Grzybowski, E. A. Feilat, P. Knight and L. Doriott, Breakdown voltage behavior of PET thermoplastics at DC and AC voltages, *Proc. IEEE Southeastcon'99. Technology on the Brink of 2000* (1999), pp. 284–287.
- ¹⁸K. Elanseralathan, M. J. Thomas and G. R. Nagabhushana, Breakdown of solid insulating materials under high frequency high voltage stress, *Proc. 6th Int. Conf. Properties and Applications of Dielectric Materials* (1999), pp. 999–1001.
- ¹⁹T. Tanaka, M. Kozako, N. Fuse and Y. Ohki, Proposal of a multi-core model for polymer nanocomposite dielectrics, *IEEE Trans. Dielectr. Electr. Insul.* **12**(4), 669–681 (2005).
- ²⁰T. J. Lewis, Interfaces are the dominant feature of dielectrics at the nanometric level, *IEEE Trans. Dielectr. Electr. Insul.* **11**(5), 739–753 (2004).
- ²¹J. B. Hasted, D. M. Ritson and C. H. Collie, Dielectric properties of aqueous ionic solutions. *Parts I and II*, *J. Chem. Phys.* **16**, 1 (1948).
- ²²N. Gavish and K. Promislow, Dependence of the dielectric constant of electrolyte solutions on ionic concentration., *Phys. Rev.* **94**, 1 (2016).